Acylglycerol kinase contributes to cell proliferation by activating NF-κB signaling pathway in pancreatic cancer

KUNKUN HAN[1,2*], QIANYUN ZHANG[1,3*], SHENGNAN GAO[1*], JIGANG ZHANG[4], XIAO MEI[2], FEI LI[1,3], XIN XU[2,5], SHU LI[1] and GUODONG CHEN[1-3]

[1]School of Basic Medical Sciences, Wannan Medical College, Wuhu, Anhui 241002, P.R. China; [2]Center for Self-Propelled Nanotechnologies, College of Biotechnology, Suzhou Industrial Park Institute of Services Outsourcing, Suzhou, Jiangsu 215125, P.R. China; [3]Anhui Province Key Laboratory of Basic Research and Transformation of Age-Related Diseases, Wannan Medical College, Wuhu, Anhui 241002, P.R. China; [4]Department of Emergency Medicine, The First Affiliated Hospital of Soochow University, Suzhou, Jiangsu 215006, P.R. China; [5]Translational Cancer Research Laboratory, Suzhou Acumen Medical Technology, Suzhou, Jiangsu 215123, P.R. China

Received November 19, 2025; Accepted April 2, 2026

DOI: 10.3892/or.2026.9145

Abstract. Pancreatic cancer mortality remains high due to late diagnosis and therapeutic resistance. The present study investigated acylglycerol kinase (AGK), which has been implicated in other tumors, in pancreatic cancer. Quantitative PCR, western blotting and immunohistochemistry analyses showed that AGK was markedly upregulated in pancreatic cancer tissues and cell lines and its expression associated with poor prognosis. Furthermore, functional studies using AGK knockdown and overexpression models demonstrated that AGK promoted cancer cell proliferation by upregulating proliferation-associated genes, such as *MYC*, *MKI67* and *CCNB1*. Mechanistically, AGK activates NF-κB signaling pathway by facilitating p65 nuclear translocation and enhancing its phosphorylation. Additionally, CCK-8 and colony formation assays further indicated that elevated AGK levels reduced sensitivity to therapeutic drugs and irradiation in pancreatic cancer cells. These findings revealed the critical role of AGK in pancreatic cancer progression and treatment resistance, identifying it as a potential novel therapeutic target and diagnostic marker.

Correspondence to: Professor Shu Li or Professor Guodong Chen, School of Basic Medical Sciences, Wannan Medical College, Higher Education Park, 22 Wenchang West Road, Wuhu, Anhui 241002, P.R. China
E-mail: wylishu@wnmc.edu.cn
E-mail: c3024034@163.com

*Contributed equally

Key words: acylglycerol kinase, cell proliferation, pancreatic cancer, NF-κB

Introduction

Pancreatic cancer ranks as the 12th most common malignancy and the seventh leading cause of cancer-related deaths worldwide (1). Its high mortality has earned it the designation 'king of cancers'. Due to the absence of early symptoms and therapy resistance, the 5-year survival rate for pancreatic cancer remains only ~10%, with a median overall survival of 9.3 months (2). Notably, the incidence of pancreatic cancer has increased annually. It is estimated that pancreatic cancer will become the second leading cause of cancer death by 2030 in the USA (3). In China, the incidence has risen sharply from 26.77 thousand cases in 1990 to 114.96 thousand in 2019, and is projected to reach 218.79 thousand by 2030, representing an approximate two-fold increase (4). Currently, chemotherapy is the most frequently used approach for most patients with pancreatic cancer, owing to the frequent presentation of metastatic or unresectable disease at diagnosis (5). Other therapeutic approaches including surgery, radiotherapy, immunotherapy, and targeted therapy, are employed depending on the cancer stage (6). However, the effectiveness of all available treatments remains unsatisfactory (7). Hence, there is an urgent need to discover novel targets or strategies for pancreatic cancer treatment.

Acylglycerol kinase (AGK) is a lipid kinase that catalyzes the phosphorylation of acylglycerol to produce lysophosphatidic acid (8). Growing evidence indicates that AGK acts as an oncogene, being upregulated in various cancers and promoting tumor progression (9). Zhu *et al* (10) found that AGK upregulation in nasopharyngeal carcinoma patients is associated with lymph node metastasis and poor prognosis. In cervical squamous cell carcinoma cells, high AGK expression enhances epithelial-mesenchymal transition by inducing hypoxia-inducible factor 1 α expression (11). AGK also activates the PI3K/AKT/glycogen synthase kinase-3 beta (GSK3β) signaling pathway, thereby promoting tumor growth and metastasis in renal cell carcinoma (12). Overexpression of AGK leads to constitutive activation of JAK2/STAT3 signaling

and promotes the proliferation of esophageal squamous cell carcinoma (13). In addition, plasma membrane-localized AGK has been reported to suppress phosphatase and tensin homolog (PTEN) phosphorylation, enhancing antitumor immunity by promoting CD8+ T cell proliferation (14). However, the expression and biological functions of AGK in pancreatic cancer remain unclear.

The present study demonstrated that AGK is markedly upregulated in pancreatic cancer and correlates with shorter overall survival. Furthermore, it showed that AGK upregulates the expression of proliferation-related genes, such as *MKI67* and *CCNB1*, resulting in accelerated cell proliferation. Importantly, the results indicated that AGK activates the NF-κB signaling pathway by promoting the phosphorylation of NF-κB p65. Moreover, AGK upregulation confers resistance to both chemotherapeutic agents and radiation in human pancreatic cancer cells. These findings provide new insights into the functions of AGK in pancreatic cancer and suggest that targeting AGK may represent a novel therapeutic or diagnostic strategy.

Materials and methods

Cells, tissues and chemicals. The normal human pancreatic ductal epithelial cell line HPDE6-C7 and four pancreatic cancer cell lines (AsPC-1, BxPC-3, Capan-2 and PANC-1) were purchased from the American Type Culture Collection. All cells were cultured in RPMI-1640 medium (HyClone™; Cytiva) supplemented with 10% fetal bovine serum (FBS; BioChannel Biological Technology Co., Ltd.), 100 U/ml penicillin, and 100 μg/ml streptomycin, and maintained at 37˚C in a humidified incubator with 5% CO_2. A total of 16 paired pancreatic cancer and matched adjacent non-cancerous tissue samples (collected ≤2 cm away from the tumor margin) were collected from patients diagnosed with pancreatic cancer between January 2025 and June 2025. Of the 16 enrolled patients, nine were male and seven were female, with a median age of 62 years (age range: 45-78 years). This study was approved by the Institutional Ethics Committee of Wannan Medical College (approval no. 245), and written informed consent was obtained from all participants. Nab-paclitaxel, gemcitabine, and NF-κB inhibitor (N4-[2-(4-phenoxyphenyl)ethyl]-1,2-dihydroquinazoline-4,6-diamine, EVP4593 (QNZ) were purchased from Selleck Chemicals.

Bioinformatics analyses. AGK expression in pancreatic cancer was analyzed using Gene Expression Profiling Interactive Analysis 2 (GEPIA2), an online tumor database (version 2.0; http://gepia2.cancer-pku.cn/) that integrates The Cancer Genome Atlas (TCGA) tumor, TCGA normal and Genotype-Tissue Expression (GTEx) normal tissue data (http://gepia2.cancer-pku.cn/#analysis) and all analyses were performed with default parameters. Overall survival analysis of AGK in pancreatic cancer was also conducted via GEPIA2 (http://gepia2.cancer-pku.cn/#survival) using default settings. To further assess the prognostic significance of AGK across tumor stages, a stratified survival analysis was conducted using the Kaplan-Meier Plotter online tool (https://kmplot.com/analysis/), utilizing integrated TCGA and Gene Expression Omnibus (GEO) data. Pancreatic cancer cases were categorized into early-stage (I+II) and advanced-stage (III+IV) groups based on AJCC criteria. Within each stage subgroup, patients were dichotomized into high- and low-AGK expression groups using the median expression value. Kaplan-Meier curves were plotted, and overall survival differences were evaluated with the log-rank test.

Correlation analysis between AGK expression and proliferation-related gene expression in pancreatic cancer was performed using the GEPIA2 database. For this analysis, the analysis was restricted to all pancreatic cancer tumor samples included in the GEPIA2 database, and the expression level of AGK matched with that of four target proliferation-associated genes (MKI67, CCNB1, CCND1 and MYC). Pearson correlation coefficient was calculated to evaluate the association between gene expression levels, and the visualization results generated by the database were exported for the present study.

Reverse transcription-quantitative (RT-q) PCR. Total RNA was extracted from approximately $1x10^6$ cells per sample using RNAiso Plus (Takara Biotechnology Co., Ltd.) according to the manufacturer's protocol. First-strand cDNA was synthesized from 1 μg of total RNA using the PrimeScript RT reagent Kit (Takara Biotechnology Co., Ltd.) strictly following the manufacturer's instructions. qPCR was performed with the TB Green Premix Ex Taq II kit (Takara Biotechnology Co., Ltd.) on a LightCycler 480 real-time PCR system (Roche Diagnostics) in accordance with the manufacturer's protocol. The PCR cycling conditions were as follows: initial denaturation at 95˚C for 30 sec, followed by 40 cycles of denaturation at 95˚C for 5 sec and annealing/extension at 60˚C for 30 sec. The sequences of primers used for qPCR are listed in Table I. Relative mRNA levels were calculated using the $2^{-\Delta\Delta Cq}$ method (15), and data were normalized to the internal reference gene *GAPDH* (16). All qPCR experiments were performed in at least three independent biological replicates.

Plasmids, siRNAs and transfection. The full-length coding sequence of human AGK was amplified by PCR, and cloned into the pcDNA3.1 vector to generate an N-terminal Flag-tagged AGK overexpression plasmid. For transfection performed in standard 6-well culture plates, 2 μg of constructed plasmid (per well) was used for overexpression experiments, and the final working concentration of siRNA was 50 nM (per well) for knockdown experiments. Negative control siRNA (si-NC) and AGK-targeting siRNA (si-AGK) were synthesized by Sangon Biotech Co., Ltd.. Plasmids were transfected using Lipofectamine® 2000 (Invitrogen; Thermo Fisher Scientific, Inc.) and siRNAs were transfected with Lipofectamine® RNAiMAX (Invitrogen; Thermo Fisher Scientific, Inc.), following the manufacturers' protocols. All transfection reactions were incubated at 37˚C in a humidified 5% CO_2 incubator for 4-6 h, before transfection medium was replaced with fresh complete culture medium. Subsequent downstream experiments were carried out 48 h after siRNA transfection, and 24-48 h after plasmid transfection. The siRNA sequences are as follows: si-AGK: 5'-AAC AGA TGA GGC TAC CTT CAG-3'; si-NC: 5'-TTC TCC GAA CGT GTC ACG T-3'.

Table I. Primers for reverse transcription-quantitative PCR

Target gene	Primer	Sequence (5'-3')
AGK	Forward	CTTGACAGGCTGCTCTCCTT
	Reverse	GGAAGAAAACTACAGCTGGGC
MYC	Forward	GGCTCCTGGCAAAAGGTCA
	Reverse	CTGCGTAGTTGTGCTGATGT
MKI67	Forward	CTTTGGGTGCGACTTGACG
	Reverse	GTCGACCCCGCTCCTTTT
CCNB1	Forward	AATAAGGCGAAGATCAACATGGC
	Reverse	TTTGTTACCAATGTCCCCAAGAG
GAPDH	Forward	GCACCGTCAAGGCTGAGAAC
	Reverse	TGGTGAAGACGCCAGTGGA

Nuclear and cytoplasmic fractionation. Subcellular fractionation was performed using the Beyotime Nuclear and Cytoplasmic Protein Extraction Kit (Beyotime Biotechnology) according to the manufacturer's instructions. Briefly, harvested cells were washed with ice-cold phosphate-buffered saline (PBS) and lysed in hypotonic Reagent A supplemented with protease inhibitors. Following the addition of Reagent B, cytoplasmic proteins were isolated in the supernatant after centrifugation (15,000 x g, 5 min, 4˚C). The nuclear pellet was subsequently lysed in high-salt Reagent C (30 min on ice with intermittent vortexing) and clarified by centrifugation (15,000 x g, 10 min, 4˚C) to obtain the nuclear fraction. Fraction purity was verified by western blotting with antibodies against GAPDH (a cytoplasmic marker) and histone H3 (a nuclear marker).

Western blotting. Western blotting was performed as previously described (16,17). Total protein was extracted using ice-cold RIPA lysis buffer (Beyotime Biotechnology) supplemented with 1% (v/v) 100 mM phenylmethylsulfonyl fluoride and 1% (v/v) phosphatase inhibitor cocktail (MedChemExpress). Protein concentration was determined with the bicinchoninic acid protein assay kit (Thermo Fisher Scientific, Inc.) following the manufacturer's instructions. Equal amounts of protein (30 μg per lane) were separated by 10% sodium dodecyl sulfate-polyacrylamide gel electrophoresis, then transferred onto 0.4 μm polyvinylidene difluoride membranes (MilliporeSigma). Membranes were blocked with 5% (w/v) non-fat dry milk (Bio-Rad Laboratories, Inc.) in Tris-buffered saline with 0.1% Tween 20 (TBST) for 1 h at room temperature. All primary antibodies were diluted and incubated overnight at 4˚C: Anti-Flag (1:1,000; Medical & Biological Laboratories Co., Ltd.), anti-GAPDH (1:5,000; Proteintech Group, Inc.), anti-IκBα (1:1,000; Proteintech Group, Inc.), anti-IKKα/β (1:1,000; MedChemExpress), anti-histone H3 (1:1,000; MedChemExpress), anti-AGK (1:1,000; Santa Cruz Biotechnology, Inc.), anti-phospho-p65 (1:1,000; Cell Signaling Technology, Inc.), anti-phospho-IKKα/β (1:1,000; Cell Signaling Technology, Inc.), anti-phospho-IκBα (1:1,000; Cell Signaling Technology, Inc.), anti-p65 (1:1,000; Cell Signaling Technology, Inc.). After washing, membranes were incubated with HRP-conjugated secondary antibodies (goat anti-rabbit IgG, 1:5,000; goat anti-mouse IgG, 1:5,000; Beyotime Biotechnology) for 1 h at room temperature. Protein bands were visualized using enhanced chemiluminescence visualization reagent (MilliporeSigma).

Cell growth and viability assay. Cell viability was assessed using the Cell Counting Kit-8 (CCK-8; Selleck Chemicals), as described previously (18). In brief, cells were seeded in 96-well plates at a density of 2,000 cells per well and cultured at 37˚C in a 5% CO_2 humidified incubator for 1, 2, and 4 days. Then, 10 μl of CCK-8 reagent was added to each well and incubated for 2 h at 37˚C. Absorbance was measured at 450 nm using a SpectraMax i3 microplate reader (Molecular Devices, LLC.).

Wound healing assay. Wound healing assays were performed as previously described (19). Briefly, cells in the logarithmic growth phase were enzymatically detached and resuspended at 2x10^6 cells/ml. A total of 2x10^6 cells (in 1 ml of suspension) were seeded into each well of a 6-well plate. Then, 1 ml of complete medium (supplemented with 10% FBS) was added to each well, and the cells were cultured until they reached ~90 confluence (~18 h). Uniform wounds were created using 10 μl sterile pipette tips, followed by three washes with PBS. After replacing the medium with serum-free medium, wound images were captured immediately (T_0) and at 48 h (T_{48}). The percentage of wound closure was calculated using the formula: $[(A_0-A_{48})/A_0]$ x 100%, where A represents the wound area.

Transwell migration assay. Cell migration was assessed using Transwell chambers as previously described (20). Briefly, 2.5x10^4 cells in serum-free medium were seeded into the upper chamber of a Transwell insert (8.0 μm pore size; Corning, Inc.). The lower chamber was filled with medium containing 10% FBS as a chemoattractant. After incubation for 24 h at 37˚C, non-migrated cells on the upper surface of the membrane were gently wiped off with cotton swabs. Cells that had migrated to the lower surface were fixed with 100% methanol for 15 min, stained with 0.1% crystal violet for 20 min at room temperature (22-24˚C), and rinsed gently with PBS. The membranes were then imaged under phase-contrast microscopy (Nikon Corporation). Migrated cells were quantified by counting the number of cells in five randomly selected fields per membrane at 200x magnification.

Colony formation assay. For assessment of clonogenic ability, transfected cells (300 cells per well) were seeded in 6-well plates and cultured in DMEM supplemented with 10% FBS at 37˚C in a humidified atmosphere containing 5% CO_2. After 10 days, cells were washed with ice-cold PBS, fixed in 4% paraformaldehyde for 30 min at room temperature and stained with 0.1% crystal violet solution for 30 min at room temperature (22-24˚C). After gentle rinsing with distilled water and air-drying, the number of colonies containing ≥50 cells was counted and representative images were captured.

For evaluation of radiosensitivity, PANC-1 cells transfected with empty vector (EV) or Flag-AGK overexpression plasmids were irradiated with X-rays at doses of 0, 2, 4 and 6 Gy. Cells were then cultured at 37˚C in a 5% CO_2 humidified incubator for 14 days to allow colony formation. Colonies were fixed,

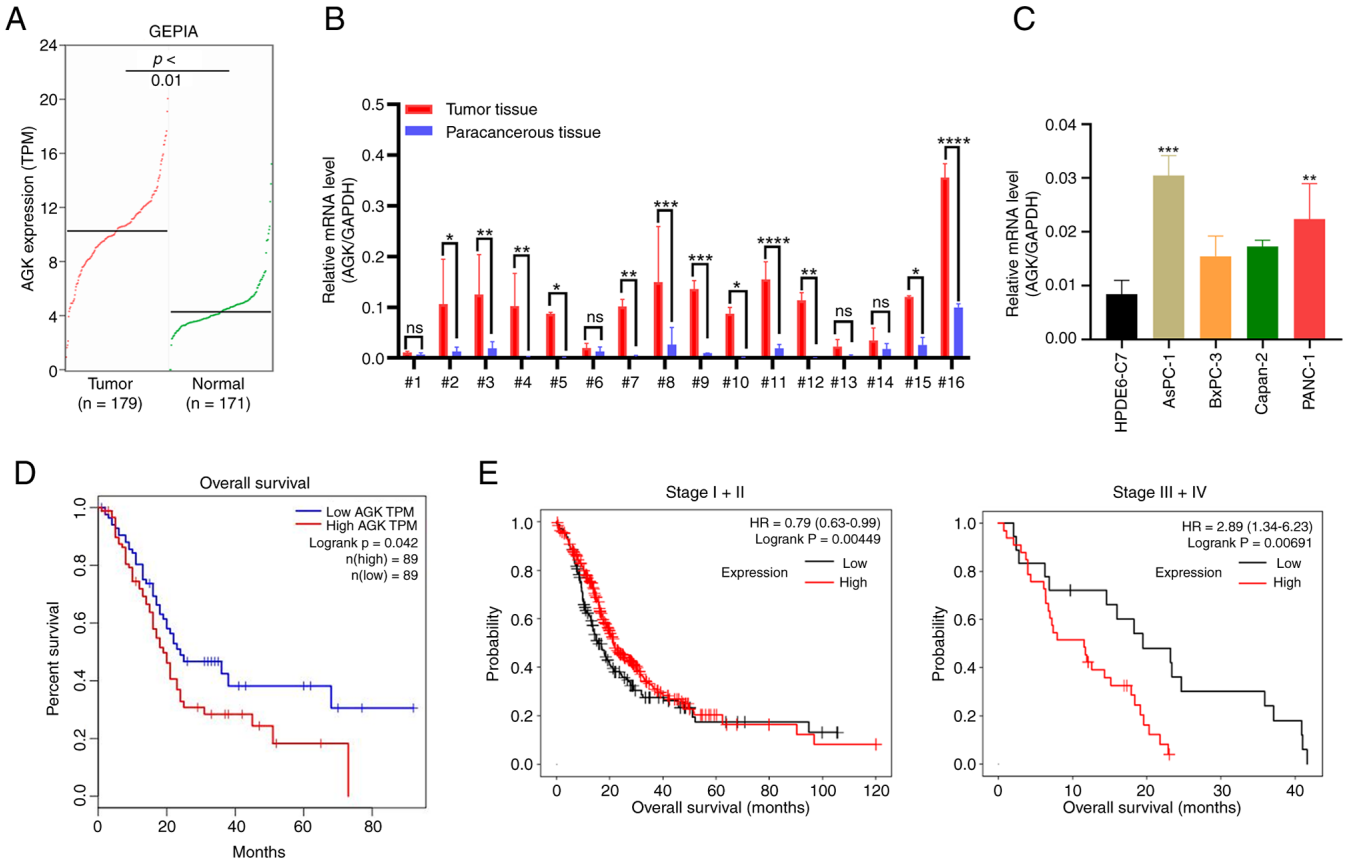

Figure 1. AGK is upregulated in pancreatic cancer and correlates with poor prognosis. (A) AGK expression in PAAD and normal tissues was analyzed using the GEPIA database. (B) AGK expression were detected in sixteen pairs of tumorous and adjacent non-tumor tissues by qPCR, with GAPDH as an internal control. (C) AGK expression was measured in a normal human pancreatic ductal epithelial cell line (HPDE6-C7) and four pancreatic cancer cell lines using qPCR. (D) Overall survival analysis was performed using the GEPIA online database. (E) Kaplan-Meier overall survival curves of pancreatic cancer patients stratified by AGK expression level (low vs. high) and tumor stage. Left panel: Early-stage (Stage I+II) disease; right panel: Advanced-stage (Stage III+IV) disease. Data are mean ± SD, *P<0.05, **P<0.01, ***P<0.001, ****P<0.0001. AGK, acylglycerol kinase; PAAD, pancreatic adenocarcinoma; GEPIA, Gene Expression Profiling Interactive Analysis; qPCR, quantitative PCR; HR, hazard ratio.

stained, and counted as aforementioned. The surviving fraction at each dose was calculated, and the survival fraction at 2 Gy was recorded as SF_2, a standard indicator of cellular radiosensitivity. Cell survival curves were fitted using a single-hit multi-target model in GraphPad Prism 8 (Dotmatics). The sensitization enhancement ratio (SER) was calculated at the 37% survival fraction (SER_{37}).

Xenograft models. PANC-1 cells ($3x10^6$ cells per injection site) were inoculated into the right flank of each female BALB/c nude mouse aged 6-8 weeks. The total number of experimental animals was 10 (5 individuals per group; 2 groups in total), and the average body weight of mice at inoculation was 18-22 g. All animals were purchased from GemPharmatech Co., Ltd. Mice were housed in specific pathogen-free facilities with the following standardized rearing conditions: ambient temperature 20-24˚C, relative humidity 40-60%, 12-h light/dark cycle, with free access to sterile food and water. When tumors became palpable and reached a volume of ~50 mm^3, mice were randomly divided into two groups (n=5 per group) using a random number table, and intratumorally injected with indicated siRNAs complexed with *in vivo*-jetPEI Delivery Reagent (Polyplus-transfection Inc.) every 7 days. Tumor volume was calculated using the standard formula: Volume=(length x $width^2$)/2, and was measured every 3 days for 3 consecutive weeks. To minimize observation bias, tumor measurements and assessments were performed by personnel blinded to group assignments. On Day 21, mice were sacrificed and tumors were excised for further analysis.

All experimental animals were sacrificed via carbon dioxide (CO_2) inhalation in accordance with the AVMA Guidelines for the Euthanasia of Animals (2020 Edition; available at: https://www.avma.org/sites/default/files/2020-01/2020-Euthanasia-Final-1-17-20.pdf). No additional chemical agents were administered to animals prior to sacrifice. For CO_2-induced euthanasia, the volume displacement rate was set at 40% of the euthanasia chamber volume per minute. Mortality was confirmed by the absence of spontaneous breathing, loss of corneal reflex, and no response to toe pinch stimulation.

Dual-luciferase reporter assay. An NF-κB-driven luciferase reporter plasmid was purchased from Beyotime Biotechnology. PANC-1 and AsPC-1 cells were co-transfected with the NF-κB luciferase reporter plasmid, the internal control *Renilla* luciferase plasmid and the indicated experimental plasmids or siRNAs using Lipofectamine® 2000 Transfection Reagent (Thermo Fisher Scientific, Inc.). After 48 h of incubation post-transfection, luciferase activity was measured using the Dual-Luciferase® Reporter Assay System (Promega

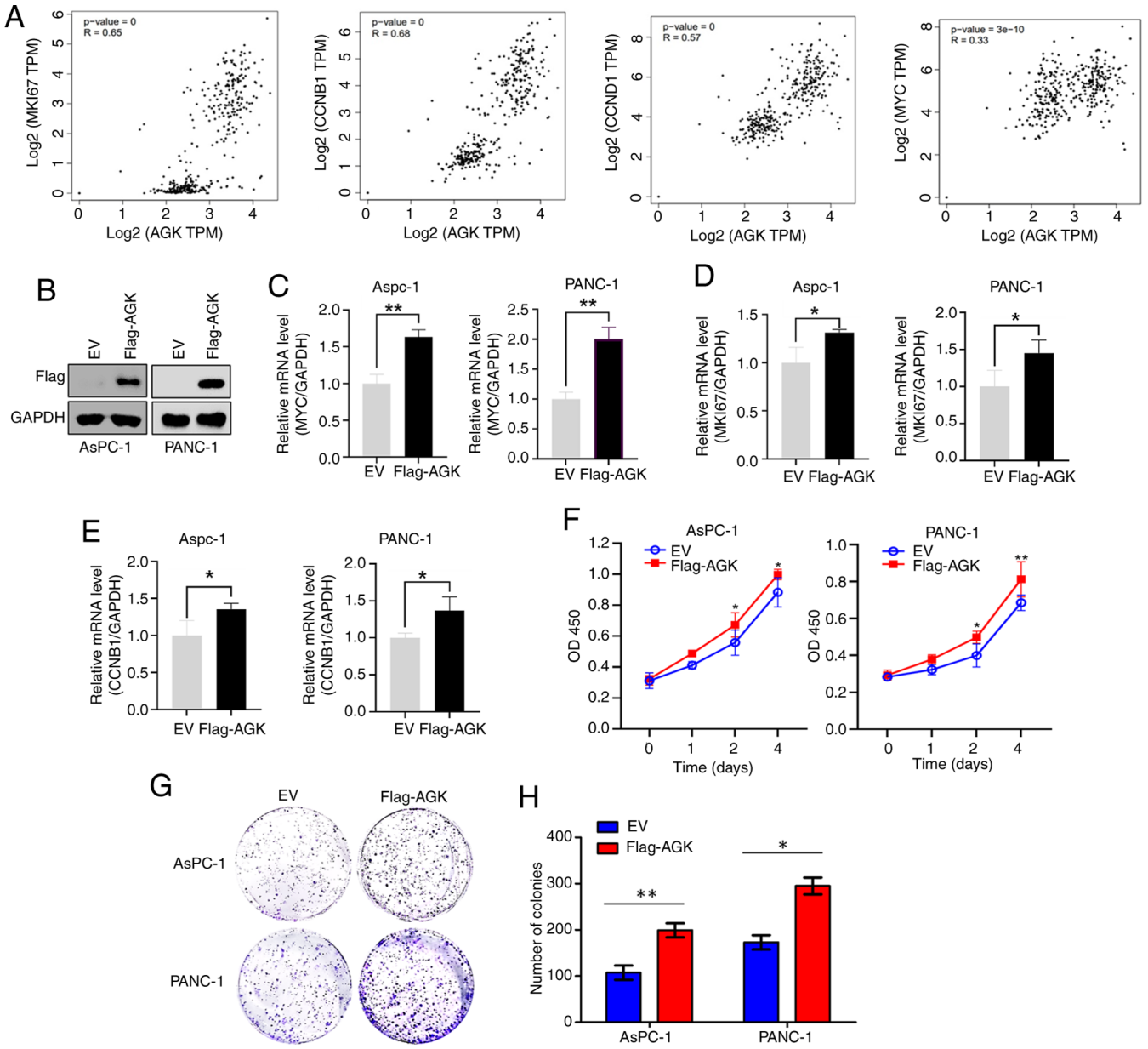

Figure 2. AGK promotes the proliferation of pancreatic cancer cells. (A) Correlation analysis between AGK expression and *MKI67*, *CCNB1*, *CCND1* or *MYC* was performed using the GEPIA database. (B) AGK protein levels were measured in AsPC-1 and PANC-1 cells transfected with EV or AGK-overexpressing plasmids (Flag-AGK) by western blot analysis using an anti-Flag antibody. GAPDH served as a loading control. AsPC-1 and PANC-1 cells were transfected with EV or Flag-AGK plasmids for 48 h, followed by qPCR analysis of (C) *MYC*, (D) *MKI67* and (E) *CCNB1* expression. GAPDH was used as an internal control. (F) The viability of AsPC-1 and PANC-1 cells transfected with indicated plasmids was assessed at indicated time points by CCK-8 assay. (G) Representative crystal violet-stained colonies of AsPC-1 and PANC-1 cells transfected with EV or Flag-AGK. (H) Quantification of colony numbers from three independent experiments (mean ± SD). Data are representative of three independent experiments. *P<0.05, **P<0.01. AGK, acylglycerol kinase; GEPIA, Gene Expression Profiling Interactive Analysis; EV, empty vector; qPCR, quantitative PCR.

Corporation) according to the manufacturer's instructions. Firefly luciferase activity was normalized to the *Renilla* luciferase activity to calculate the relative NF-κB activity.

Statistical analysis. All experiments were performed in at least three independent biological replicates. Data are presented as the mean ± standard deviation (SD). Differences between two groups were compared using Student's t-test and comparisons among three or more groups were performed with one-way or two-way ANOVA followed by Tukey's post hoc test for multiple comparisons. All plots and graphs were generated using GraphPad Prism version 8.0.2 (Dotmatics).

Results

AGK is upregulated and correlates with poor prognosis in pancreatic cancer. To investigate the role of AGK in pancreatic cancer, the present study analyzed its expression levels in pancreatic cancer tissues and normal tissues based on TCGA and GTEx data using GEPIA2. AGK expression was markedly higher in tumor tissues compared to normal tissues (Fig. 1A). Validation in clinical samples showed that AGK expression was elevated in tumor tissues relative to matched adjacent non-tumor tissues in 12 of 16 patients (Fig. 1B). Consistently, AGK expression was also upregulated in various pancreatic

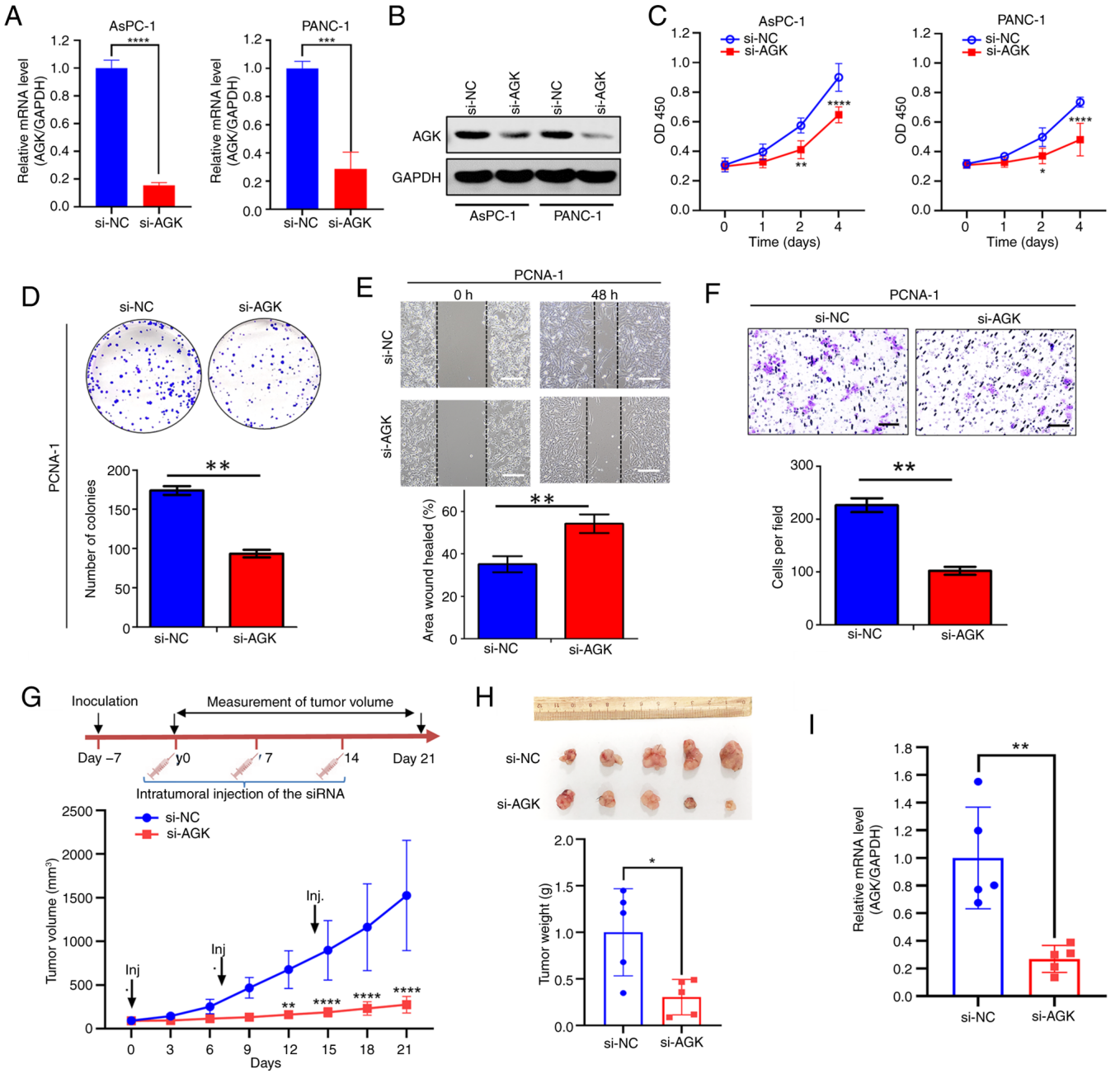

Figure 3. Knockdown of AGK inhibits cell growth of pancreatic cancer. AGK knockdown efficiency was validated in AsPC-1 and PANC-1 cells transfected with control (si-NC) or AGK-targeting (si-AGK) siRNAs by (A) qPCR and (B) western blot analyses. (C) Cell viability was measured by CCK-8 assay in AsPC-1 and PANC-1 cells after AGK knockdown. (D) Colony formation assay of PANC-1 cells transfected with si-NC or si-AGK. Upper: representative crystal violet staining images; lower: quantification of colony numbers. (E) Wound healing assay for migration of PANC-1 cells with or without AGK knockdown. Upper: Representative wound images at 0 h and 48 h; lower: Quantification of wound healing percentage. Scale bars, 200 μm. (F) Transwell invasion assay of PANC-1 cells transfected with si-NC or si-AGK. Upper: Representative staining images of invaded cells; lower: Quantification of invaded cells per field. Scale bars, 200 μm. (G) *In vivo* tumor growth assay. PANC-1 xenograft-bearing mice were intratumorally injected with si-NC or si-AGK on days 0, 7, and 14 (arrows). Tumor volumes were measured every three days. (H) Tumors were excised and weighed at the endpoint (day 21). (I) AGK mRNA levels in harvested tumors were analyzed by qPCR. Data are mean ± SD, *P<0.05, **P<0.01, ***P<0.001, ****P<0.0001. AGK, acylglycerol kinase; si, short interfering; NC, negative control; qPCR, quantitative PCR.

cancer cell lines, particularly in AsPC-1 and PANC-1 cells, relative to the normal cell line HPDE6-C7 (Fig. 1C). Survival analysis indicated that patients with high AGK expression had markedly shorter overall survival (Fig. 1D). These findings demonstrated AGK overexpression in pancreatic cancer and its potential as a prognostic marker. To further investigate the clinical relevance of AGK, the present study performed a stratified survival analysis based on tumor stage (Fig. 1E). In early-stage (stage I+II) disease, the prognostic correlation between high AGK expression and overall survival did not reach statistical significance. By contrast, in advanced-stage (stage III+IV) patients, high AGK expression was markedly associated with shorter overall survival. These results indicate that AGK plays a more prominent role in driving the progression and aggressiveness of advanced pancreatic cancer.

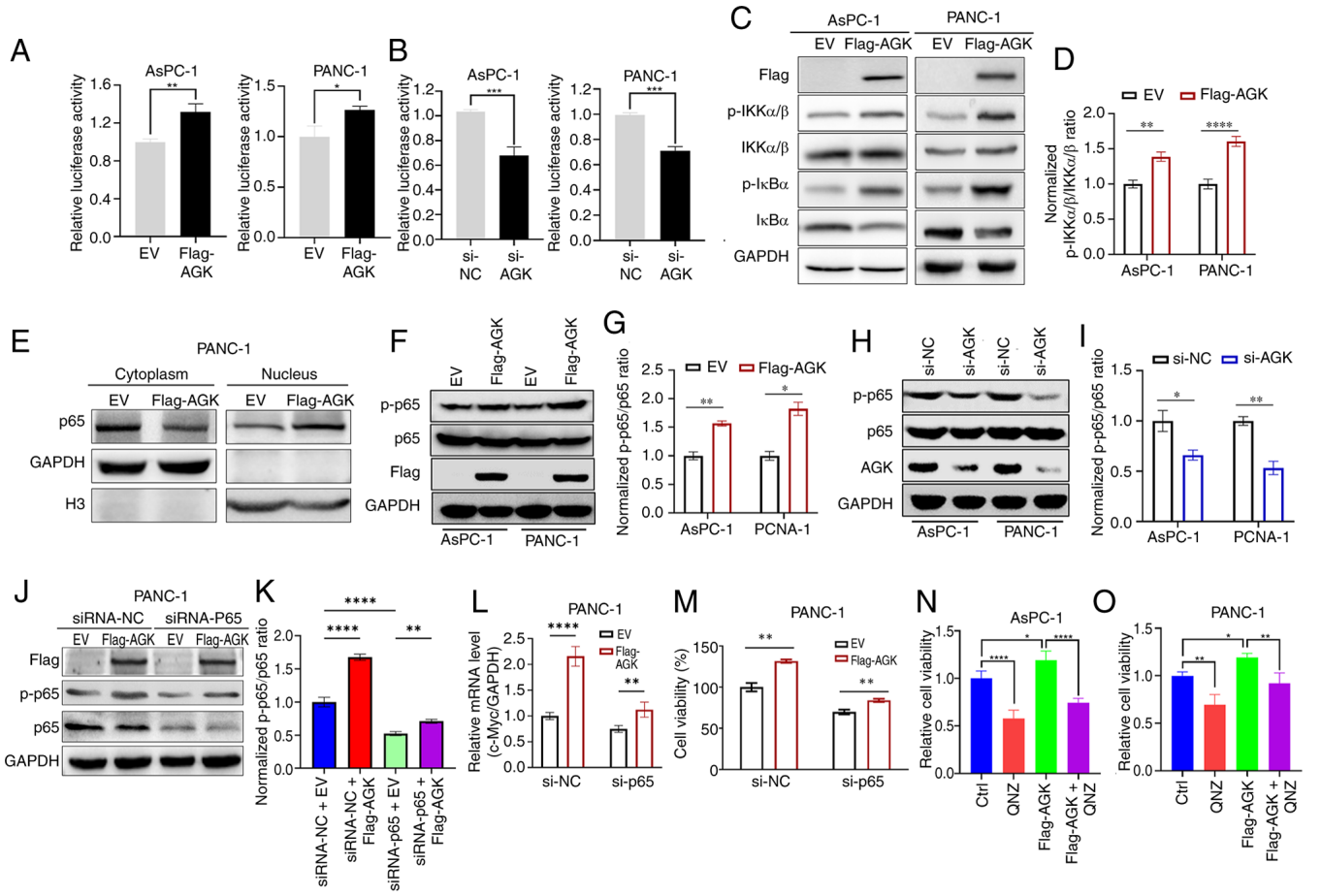

Figure 4. AGK exerts its function by regulating NF-κB signaling. AsPC-1 and PANC-1 cells harboring NF-κB-driven luciferase reporter were transfected with (A) AGK-overexpressing plasmids or (B) AGK-targeting siRNAs for 48 h, followed by dual-luciferase assay. (C) Representative western blots showing Flag-AGK, p-IKKα/β, total IKKα/β, p-IκBα, total IκBα, and GAPDH in AsPC-1 (left) and PANC-1 (right) cells transfected with EV or Flag-AGK. (D) Quantitative analysis of the normalized ratio of phosphorylated IKKα/β (p-IKKα/β) to total IKKα/β from panel C. (E) Representative western blots showing p65 subcellular localization in cytoplasmic and nuclear fractions of cells transfected with EV or Flag-AGK. GAPDH (cytosolic) and H3 (nuclear) served as loading controls. (F) Representative western blotting results of p-p65 and total p65 in AGK-overexpressing AsPC-1 and PANC-1 cells. (G) Quantitative analysis of the normalized ratio of phosphorylated p65 (p-p65) to total p65 from panel F. (H) Representative western blotting results of p-p65 and total p65 in AGK-knockdown AsPC-1 and PANC-1 cells. (I) Quantitative analysis of the normalized ratio of phosphorylated p65 (p-p65) to total p65 from panel H. (J) Western blot showing that p65 knockdown (si-p65) abolishes AGK-induced p65 phosphorylation. (K) Quantitative analysis of the normalized ratio of phosphorylated p65 (p-p65) to total p65 from panel J. (L) qPCR analysis showing that AGK-mediated upregulation of MYC mRNA is dependent on p65. (M) CCK-8 assay demonstrating that p65 knockdown attenuated AGK-induced cell proliferation. (N) AsPC-1 and (O) PANC-1 cells overexpressed with AGK were incubated with vehicle or 0.5 μM QNZ for 48 h, followed by CCK-8 assay. Data were presented as mean ± SD. *P<0.05, **P<0.01, ***P<0.001, ****P<0.0001. AGK, acylglycerol kinase; p-, phosphorylated; EV, empty vector; si, short interfering; NC, negative control; qPCR, quantitative PCR; QNZ., N4-[2-(4-phenoxyphenyl)ethyl]-1,2-dihydroquinazoline-4,6-diamine.

AGK promotes pancreatic cancer cell proliferation. Using GEPIA database, the present study found a strong positive correlation between AGK expression and that of proliferation-associated genes, including *MKI67*, *CCNB1*, *CCND1* and *MYC* (Fig. 2A). To further validate these findings, AsPC-1 and PANC-1 cells were transfected with either an EV or Flag-tagged AGK-overexpressing plasmids (Flag-AGK) (Fig. 2B). AGK overexpression markedly increased the mRNA levels of *MYC*, *MKI67*, and *CCNB1* (Fig. 2C-E). Accordingly, CCK-8 assays demonstrated accelerated proliferation in AGK-overexpressing cells (Fig. 2F). Furthermore, colony formation assays confirmed an enhanced proliferative capacity following AGK overexpression (Fig. 2G and H). Moreover, AGK was knocked down in AsPC-1 and PANC-1 cells. The high efficiency of knockdown was confirmed by qPCR (Fig. 3A) and western blotting (Fig. 3B). AGK knockdown markedly suppressed cell proliferation, as evidenced by reduced cell viability (Fig. 3C) and decreased colony formation (Fig. 3D). Additionally, AGK knockdown impaired cell migration in both wound healing and Transwell assays (Fig. 3E and F). These *in vitro* results demonstrate a key role for AGK in pancreatic cancer cell proliferation and migration.

The pro-proliferative role of AGK was further validated *in vivo* using a xenograft mouse model. Tumor growth was markedly suppressed from day 12 onward in mice treated with AGK siRNA, compared to the control group (Fig. 3G). At the endpoint (Day 21), a significant decrease in tumor volumes and weight was observed in the si-AGK group (Fig. 3G and H). AGK expression in excised tumors was confirmed to be lower in the si-AGK group (Fig. 3I), supporting the conclusion that AGK promotes tumor proliferation *in vivo*.

AGK exerts its function by regulating NF-κB signaling. To elucidate the mechanism underlying AGK-mediated

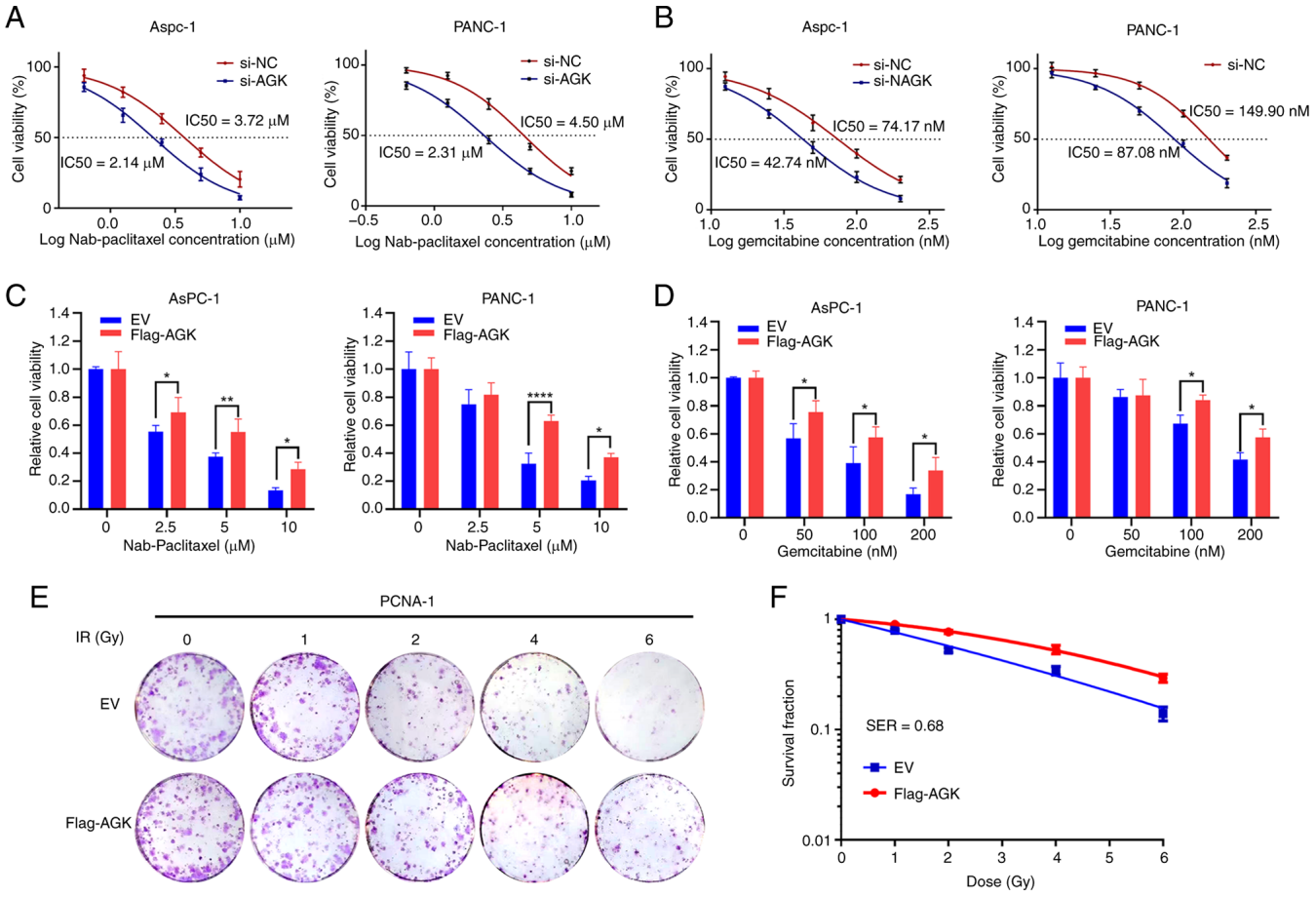

Figure 5. Response to therapeutic drugs in human pancreatic cancer cells. AsPC-1 (left) and PANC-1 (right) cells were transfected with si-NC or si-AGK, and dose-response curves along with IC_{50} values for (A) nab-paclitaxel and (B) gemcitabine were determined. The viability of AsPC-1 and PANC-1 cells overexpressing AGK was assessed after treatment with increasing concentrations of (C) nab-paclitaxel and (D) gemcitabine for 72 h by CCK-8 assay. (E) Representative images of clonogenic survival assays are shown for PANC-1 cells transfected with EV or Flag-AGK and exposure to the indicated doses of X-ray irradiation. F. Clonogenic survival fractions were calculated based on the data from (E) Data are presented as mean ± SD (n=3). *P<0.05, **P<0.01, ****P<0.0001. si, short interfering; NC, negative control; AGK, acylglycerol kinase; EV, empty vector.

tumor promotion, the present study investigated its effect on the NF-κB pathway, a key driver of pancreatic cancer proliferation (21). NF-κB reporter assays in AsPC-1 and PANC-1 cells showed that AGK overexpression markedly increased luciferase activity (Fig. 4A), while AGK knockdown markedly decreased it (Fig. 4B), suggesting that AGK modulates- the activation of the NF-κB pathway. Western blot analysis revealed that AGK overexpression enhanced the phosphorylation of IKKα/β (p-IKKα/β) and IκBα (p-IκBα), accompanied by reduced total IκBα levels (Fig. 4C and D), consistent with activation of the canonical NF-κB pathway. Subcellular fractionation assays further revealed that AGK overexpression enhanced p65 nuclear translocation, evidenced by markedly increased nuclear p65 and decreased cytoplasmic p65 (Fig. 4E). Moreover, AGK overexpression increased the phosphorylation of p65 without affecting total p65 levels (Fig. 4F and G), whereas AGK knockdown blocked the phosphorylation of p65 (Fig. 4H and I). It is well known that phosphorylation of p65 is a critical regulatory layer for maximizing NF-κB-driven gene expression (22). Collectively, these data demonstrated that AGK promotes p65 nuclear translocation and phosphorylation, resulting in the activation of NF-κB pathway.

To determine if AGK-mediated effects depend on NF-κB/p65, the present study performed a rescue experiment in PANC-1 cells. Cells were first transfected with control (si-NC) or p65-specific (si-p65) siRNA, followed by transfection with EV or Flag-AGK plasmid. Western blot analysis confirmed that AGK overexpression increased phosphorylated p65 (p-P65) levels in control cells, whereas si-p65 effectively depleted both total p65 and p-P65 regardless of AGK status (Fig. 4J and K). Accordingly, AGK-induced upregulation of *MYC* mRNA (Fig. 4L) and enhancement of cell viability (Fig. 4M) were markedly attenuated upon p65 knockdown. However, AGK overexpression still partially increased viability in p65-deficient cells, suggesting the involvement of additional, p65-independent mechanisms. This notion was further supported by the finding that AGK overexpression partially rescued the proliferation suppression induced by the NF-κB inhibitor QNZ (Fig. 4N and O).

AGK confers resistance to chemotherapy and radiotherapy. The present study next investigated the role of AGK in mediating chemotherapy or radiation resistance in pancreatic cancer. Given that nab-paclitaxel and gemcitabine are first-line chemotherapeutic agents for pancreatic cancer (23), the present

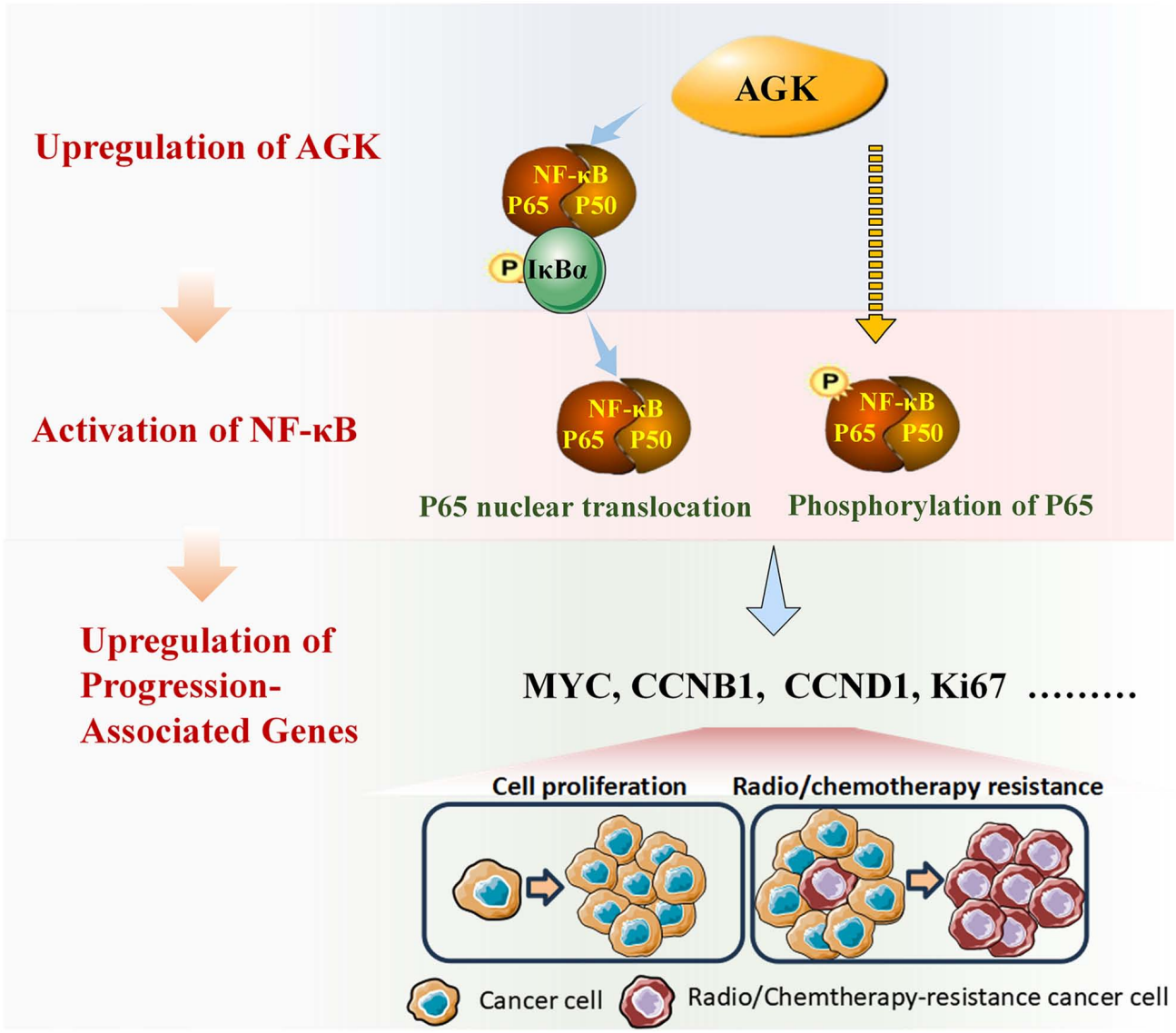

Figure 6. Schematic illustration of AGK-mediated cellular proliferation and radio/chemoresistance mechanisms. AGK upregulation promotes p65 phosphorylation at Ser536 and nuclear translocation, thereby activating NF-κB pathway. Subsequently, NF-κB pathway activation induces the expression of *MYC*, *CCNB1* and *CCND1*, which promotes tumor proliferation and confers resistance of chemotherapy and radiotherapy by enhancing cell cycle progression and survival mechanisms. AGK, acylglycerol kinase;

study first assessed their sensitivity upon modulation of AGK expression in AsPC-1 and PANC-1 cells. AGK knockdown sensitized pancreatic cancer cells to both drugs. Specifically, the IC_{50} of nab-paclitaxel decreased from ~3.72-2.14 μM in AsPC-1 cells and from ~4.50-2.31 μM in PANC-1 cells (Fig. 5A). Similarly, IC_{50} of gemcitabine decreased from ~74.17-42.74 nM in AsPC-1 cells and from ~149.90-87.08 nM in PANC-1 cells (Fig. 5B). Conversely, AGK overexpression markedly weakened the growth-inhibitory effects of both nab-paclitaxel and gemcitabine on AsPC-1 and PANC-1 cells (Fig. 5C and D). The present study then evaluated the role of AGK in radiosensitivity using a colony formation assay. AGK overexpression markedly reduced radiosensitivity, yielding an SF_2 of 0.77 and an SER_{37} of 0.68, indicating that AGK overexpression drives radioresistance in pancreatic cancer cells. (Fig. 5E and F). Collectively, these results demonstrate that AGK promotes resistance to both chemotherapy and radiotherapy in pancreatic cancer cells.

Discussion

Accumulating evidence indicates that AGK is upregulated and promotes tumor progression in various cancers. However, the signaling pathways induced by AGK vary among different cancers. AGK triggers the activation of PI3K-AKT signaling pathway in renal cell carcinoma (12) and mediates Hippo-YAP1 signaling transduction in gastric cancer (24). An earlier study also demonstrated that AGK activates NF-κB signaling pathway by increasing the phosphorylation of IKK and IκB in hepatocellular carcinoma (25). The present study confirmed that AGK promotes NF-κB activation via the canonical IKK-IκBα-p65 axis in pancreatic cancer. Moreover, the present study identified AGK as a novel regulator of p65 phosphorylation, a well-established enhancer of NF-κB activation. These findings revealed an additional layer of AGK-mediated NF-κB activation beyond canonical pathway signaling. Although NF-κB/p65 signaling is critical for AGK-driven proliferation, the partial

rescue of cell viability upon p65 knockdown or treatment with an NF-κB inhibitor suggests the involvement of complementary, p65-independent mechanisms. A limitation of the present study is the lack of systematic assessment of other potential pathways, such as PI3K/AKT or MAPK. Future work aimed at delineating the full spectrum of AGK's downstream effectors will be essential to establish a comprehensive mechanistic model and inform therapeutic strategies.

Chemoresistance remains a major cause of treatment failure in pancreatic cancer, for which chemotherapy is the mainstream treatment for the majority of unresectable cases (5,26-28). Oncogenes often contribute to such resistance and AGK has been reported to drive paclitaxel resistance in nasopharyngeal carcinoma cells (29) and sunitinib resistance in renal cell carcinoma (30). Consistent with these findings, the present data showed that AGK overexpression enhances resistance to gemcitabine and nab-paclitaxel in pancreatic cancer cells, while its knockdown markedly sensitizes cells to these agents. Together, these results suggested that targeting AGK could represent a promising therapeutic strategy and the development of specific AGK inhibitors may hold significant potential for novel drug discovery in pancreatic cancer.

The present study established AGK as an important oncogenic driver, yet several questions remain. Although NF-κB and MYC signaling are known to regulate *CCND1* and *CCNB* expression (31,32), their functional interplay within AGK-driven oncogenesis requires further investigation; particularly whether *MYC* acts as the primary downstream effector. While AGK expression is known to be transcriptionally regulated by TEAD and post-transcriptionally modulated by miRNAs (33,34), its full regulatory network remains incompletely elucidated. Moreover, the upstream mechanisms driving AGK overexpression in pancreatic cancer remain to be elucidated. Finally, the clinical relevance of AGK as a prognostic marker and therapeutic target warrants validation through large-scale, multicenter studies. Addressing these questions will be crucial for comprehensively characterizing AGK's molecular mechanisms and evaluating its translational potential in pancreatic cancer oncology.

In summary, the present study demonstrated that AGK is upregulated in pancreatic cancer and correlates with poor prognosis. Functionally, AGK promotes tumor cell proliferation *in vitro* and *in vivo*. Mechanistically, AGK activates the NF-κB pathway through two distinct mechanisms. First, it induces IκBα phosphorylation and subsequent ubiquitin-dependent degradation, leading to p65 nuclear translocation. Second, it enhances p65 phosphorylation at Ser536, thereby augmenting its transcriptional activity. Consequently, the expression of key pro-proliferative genes (e.g., *CCNB1*, *CCND1*, and *MYC*), which are regulated by p65, is increased. This AGK-driven signaling axis promotes tumor growth and confers resistance to chemotherapy and radiotherapy, likely by reinforcing cell cycle progression and survival pathways (Fig. 6). Collectively, the findings established AGK as a key driver of NF-κB-mediated tumor progression and therapy resistance, highlighting its potential as a novel therapeutic target in aggressive pancreatic cancer.

Acknowledgements

Not applicable.

Funding

The present study was supported by the Natural Science Research Project of Anhui Educational Committee (grant no. 2024AH040240), Anhui Provincial Natural Science Foundation (grant no. 2308085MH280), the High-Quality Innovation Platform of Science and Education Innovation Zone in Suzhou Industrial Park-Key Platform Project (grant no. YZCXPT2023104) and the National College Student Innovation and Entrepreneurship Training Program (grant no. 202410368075).

Availability of data and materials

The data generated in the present study are included in the figures and/or tables of this article.

Authors' contributions

Conceptualization was by KH, SL, XX and GC. Data curation was by QZ, SG, JZ and XM. Formal analysis was by KH, XX and QZ; Funding acquisition was by GC. Investigation was by KH, QZ and SG. Methodology was by XX and QZ. Project administration was by GC and SL. Resources were from KH, XX, XM and JZ. Software was by SG and FL. Supervision was by GC, XX and SL. Validation was by GC and SL. Visualization was by KH. Writing the original draft was by KH and GC. Writing, review and editing was by GC and SL. KH and GC confirm the authenticity of all the raw data. All authors read and approved the final manuscript.

Ethics approval and consent to participate

The present study was approved by the Institutional Review Board of Wannan Medical College, with approvals granted under approval no. 245 (medical ethics) and approval no. WNMC-AWE-2024440 (animal ethics). All patients signed written informed consent. Animal research was approved by the Ethics Committee of Wannan Medical College.

Patient consent for publication

Not applicable.

Competing interests

The authors declare that they have no competing interests.

References

1. Park W, Chawla A and O'Reilly EM: Pancreatic cancer: A review. JAMA 326: 851-862, 2021.
2. Li Q, Feng Z, Miao R, Liu X, Liu C and Liu Z: Prognosis and survival analysis of patients with pancreatic cancer: Retrospective experience of a single institution. World J Surg Oncol 20: 11, 2022.
3. Saad AM, Turk T, Al-Husseini MJ and Abdel-Rahman O: Trends in pancreatic adenocarcinoma incidence and mortality in the United States in the last four decades; a SEER-based study. BMC Cancer 18: 688, 2018.
4. Chen J, Chen H, Zhang T, Yin X, Man J, Yang X and Lu M: Burden of pancreatic cancer along with attributable risk factors in China from 1990 to 2019, and projections until 2030. Pancreatology 22: 608-618, 2022.

5. Lee HS and Park SW: Systemic chemotherapy in advanced pancreatic cancer. Gut Liver 10: 340-347, 2016.
6. Lin QJ, Yang F, Jin C and Fu DL: Current status and progress of pancreatic cancer in China. World J Gastroenterol 21: 7988-8003, 2015.
7. Liu B, Chen Z, Li Z, Zhao X, Zhang W, Zhang A, Wen L, Wang X, Zhou S and Qian D: Hsp90α promotes chemoresistance in pancreatic cancer by regulating Keap1-Nrf2 axis and inhibiting ferroptosis. Acta Biochim Biophys Sin (Shanghai) 57: 295-309, 2024.
8. Bektas M, Payne SG, Liu H, Goparaju S, Milstien S and Spiegel S: A novel acylglycerol kinase that produces lysophosphatidic acid modulates cross talk with EGFR in prostate cancer cells. J Cell Biol 169: 801-811, 2005.
9. Chu B, Hong Z and Zheng X: Acylglycerol Kinase-targeted therapies in oncology. Front Cell Dev Biol 9: 659158, 2021.
10. Zhu Q, Cao SM, Lin HX, Yang Q, Liu SL and Guo L: Overexpression of acylglycerol kinase is associated with poorer prognosis and lymph node metastasis in nasopharyngeal carcinoma. Tumour Biol 37: 3349-3357, 2016.
11. Ray U, Roy SS and Chowdhury SR: Lysophosphatidic acid promotes epithelial to mesenchymal transition in ovarian cancer cells by repressing SIRT1. Cell Physiol Biochem 41: 795-805, 2017.
12. Zhu Q, Zhong AL, Hu H, Zhao JJ, Weng DS, Tang Y, Pan QZ, Zhou ZQ, Song MJ, Yang JY, *et al*: Acylglycerol kinase promotes tumour growth and metastasis via activating the PI3K/AKT/GSK3beta signalling pathway in renal cell carcinoma. J Hematol Oncol 13: 2, 2020.
13. Chen X, Ying Z, Lin X, Lin H, Wu J, Li M and Song L: Acylglycerol kinase augments JAK2/STAT3 signaling in esophageal squamous cells. J Clin Invest 123: 2576-2589, 2013.
14. Hu Z, Qu G, Yu X, Jiang H, Teng XL, Ding L, Hu Q, Guo X, Zhou Y, Wang F, *et al*: Acylglycerol kinase maintains metabolic state and immune responses of CD8+ T cells. Cell Metab 30: 290-302.e5, 2019.
15. Livak K and Schmittgen TD: Analysis of relative gene expression data using real-time quantitative PCR and the 2(-Delta Delta C(T)) method. Methods 25: 402-408, 2001.
16. Xu X, Wu G, Han K, Cui X, Feng Y, Mei X, Yang P, You W and Yang Y: Inhibition of OTUB2 suppresses colorectal cancer cell growth by regulating β-Catenin signaling. Am J Cancer Res 13: 5382-5393, 2023.
17. Li Q, Zhang L, Sun Y, Du Z, Xu S, Wang X, Wei S, Tao Y, Li B, Jiang J, *et al*: p53 Modulates the Gut-Liver Axis via PI3K/AKT/Wnt Signaling Pathways in Type 2 Diabetes. FASEB J 39: e70898, 2025.
18. Wang X, Sun T, Fan J, Zuo X and Mao J: Gastrin-related circRNA_0017065 promotes the proliferation and metastasis of colorectal cancer through the miR-3174/RBFOX2 axis. Biol Direct 19: 75, 2024.
19. Yang X, Liu J, Wang C, Cheng KK, Xu H, Li Q, Hua T, Jiang X, Sheng L, Mao J and Liu Z: miR-18a promotes glioblastoma development by down-regulating ALOXE3-mediated ferroptotic and anti-migration activities. Oncogenesis 10: 15, 2021.
20. Zhu X, Wu X, Yang H, Xu Q, Zhang M, Liu X and Lv K: m6A-mediated upregulation of LINC01003 regulates cell migration by targeting the CAV1/FAK signaling pathway in glioma. Biol Direct 18: 27, 2023.
21. Carbone C and Melisi D: NF-κB as a target for pancreatic cancer therapy. Expert Opin Ther Targets 16 (Suppl 2): S1-S10, 2012.
22. Viatour P, Merville MP, Bours V and Chariot A: Phosphorylation of NF-kappaB and IkappaB proteins: Implications in cancer and inflammation. Trends Biochem Sci 30: 43-52, 2005.
23. Corrie PG, Qian W, Basu B, Valle JW, Falk S, Lwuji C, Wasan H, Palmer D, Scott-Brown M, Wadsley J, *et al*: Scheduling nab-paclitaxel combined with gemcitabine as first-line treatment for metastatic pancreatic adenocarcinoma. Br J Cancer 122: 1760-1768, 2020.
24. Huang S, Cao Y, Guo H, Yao Y, Li L, Chen J, Li J, Xiang X, Deng J and Xiong J: Up-regulated acylglycerol kinase (AGK) expression associates with gastric cancer progression through the formation of a novel YAP1-AGK-positive loop. J Cell Mol Med 24: 11133-11145, 2020.
25. Cui Y, Lin C, Wu Z, Liu A, Zhang X, Zhu J, Wu G, Wu J, Li M, Li J and Song L: AGK enhances angiogenesis and inhibits apoptosis via activation of the NF-κB signaling pathway in hepatocellular carcinoma. Oncotarget 5: 12057-12069, 2014.
26. Shimoda M, Kubota K, Shimizu T and Katoh M: Randomized clinical trial of adjuvant chemotherapy with S-1 versus gemcitabine after pancreatic cancer resection. Br J Surg 102: 746-754, 2015.
27. Long J, Zhang Y, Yu X, Yang J, LeBrun DG, Chen C, Yao Q and Li M: Overcoming drug resistance in pancreatic cancer. Expert Opin Ther Targets 15: 817-828, 2011.
28. Jin L, Qian D, Tang X, Huang Y, Zou J and Wu Z: SMYD2 imparts gemcitabine resistance to pancreatic adenocarcinoma cells by upregulating EVI2A. Mol Biotechnol 66: 2920-2933, 2024.
29. Zhao C, Chen HY, Zhao F, Feng HJ and Su JP: Acylglycerol kinase promotes paclitaxel resistance in nasopharyngeal carcinoma cells by regulating FOXM1 via the JAK2/STAT3 pathway. Cytokine 148: 155595, 2021.
30. Sun Y, Zhu L, Liu P, Zhang H, Guo F and Jin X: ZDHHC2-Mediated AGK palmitoylation activates AKT-mTOR signaling to reduce sunitinib sensitivity in renal cell carcinoma. Cancer Res 83: 2034-2051, 2023.
31. Dang CV, O'Donnell KA, Zeller KI, Nguyen T, Osthus RC and Li F: The c-Myc target gene network. Semin Cancer Biol 16: 253-264, 2006.
32. Dolcet X, Llobet D, Pallares J and Matias-Guiu X: NF-kB in development and progression of human cancer. Virchows Arch 446: 475-482, 2005.
33. Chi H: miR-194 regulated AGK and inhibited cell proliferation of oral squamous cell carcinoma by reducing PI3K-Akt-FoxO3a signaling. Biomed Pharmacother 71: 53-57, 2015.
34. Long Y, Li C and Zhu B: Circ_0008068 facilitates the oral squamous cell carcinoma development by microRNA-153-3p/acylgycerol kinase (AGK) axis. Bioengineered 13: 13055-13069, 2022.